

Modulated spin waves and robust quasi-solitons in classical Heisenberg rings

Heinz-Jürgen Schmidt*

Department of Physics, University of Osnabrück, D-49069 Osnabrück, Germany

Christian Schröder

*Department of Electrical Engineering and Computer Science,
University of Applied Sciences Bielefeld, D-33602 Bielefeld,
Germany & Ames Laboratory, Ames, Iowa 50011, USA*

Marshall Luban

*Ames Laboratory & Department of Physics and Astronomy,
Iowa State University, Ames, Iowa 50011, USA*

We investigate the dynamical behavior of finite rings of classical spin vectors interacting via nearest-neighbor isotropic exchange in an external magnetic field. Our approach is to utilize the solutions of a continuum version of the discrete spin equations of motion (EOM) which we derive by assuming continuous modulations of spin wave solutions of the EOM for discrete spins. This continuous EOM reduces to the Landau-Lifshitz equation in a particular limiting regime. The usefulness of the continuum EOM is demonstrated by the fact that the time-evolved numerical solutions of the discrete spin EOM closely track the corresponding time-evolved solutions of the continuum equation. Of special interest, our continuum EOM possesses soliton solutions, and we find that these characteristics are also exhibited by the corresponding solutions of the discrete EOM. The robustness of solitons is demonstrated by considering cases where initial states are truncated versions of soliton states and by numerical simulations of the discrete EOM equations when the spins are coupled to a heat bath at finite temperatures.

I. INTRODUCTION

With the remarkable progress in recent years in synthesizing and analyzing magnetic molecules of great diversity [1]-[3] it is timely to focus on the dynamical behavior of finite arrays of interacting spins. In this paper we direct our attention to ring structures consisting of N equally-spaced (spacing a) classical spins (unit vectors) that interact via ferromagnetic nearest-neighbor isotropic exchange and are subject to an external magnetic field $\mathbf{B} = B\mathbf{e}$. The equations of motion (EOM) of the discrete spin vectors can be written as

$$\frac{d}{dt}\mathbf{s}_n(t) = \mathbf{s}_n(t) \times (\mathbf{s}_{n-1}(t) + \mathbf{s}_{n+1}(t) + \mathbf{B}), \quad (1)$$
$$n = 0, \dots, N-1,$$

where all variables are dimensionless and the unit vectors \mathbf{s}_n are subject to the cyclic condition $\mathbf{s}_{n+N} \equiv \mathbf{s}_n$. It is well known that the solutions of Eq. (1) exhibit a wide variety of dynamical characteristics. Among these are: Exact analytical solutions, called “spin waves” [4]; numerical solutions that exhibit chaotic behavior [5]; as well as numerical solutions that are discretized versions of the soliton solutions [6] of a continuum version of Eq. (1), specifically the Landau-Lifshitz equation [7] in the case of $B \neq 0$.

The key result of this paper is that the EOM of Eq. (1) admit a wide class of numerical solutions with soliton-like characteristics. They are discretized versions of soliton solutions of a new continuum EOM that includes the Landau-Lifshitz equation as a special, limiting case. We will refer to such discretized solutions as “quasi-solitons”, using this cautious terminology since we do not know whether they correspond to strict soliton solutions of Eq. (1). A single quasi-soliton solution is a localized disturbance that propagates in the ring while for the most part maintaining its initial shape. We also find that it is possible to achieve two-quasi-soliton solutions, where a pair of initially separated single quasi-solitons collide multiple times and emerge from collisions without appreciable modification. Moreover, we identify solutions of Eq. (1) that exhibit a transition from laminar-like to turbulent-like behavior.

Our continuum EOM is obtained as follows. We recall the general spin wave solution of Eq. (1)

$$\mathbf{s}_n(t) = \begin{pmatrix} \sqrt{1-z^2} \cos(qn - Bt - \omega t) \\ \sqrt{1-z^2} \sin(qn - Bt - \omega t) \\ z \end{pmatrix}, \quad (2)$$

where

$$q = \frac{2\pi k}{N}, \quad (k = 0, \dots, N-1) \quad (3)$$

the angular frequency ω is given by

$$\omega = 2(1 - \cos q)z \quad (4)$$

*Electronic address: hschmidt@uos.de

and z is an arbitrary real number in the interval $-1 < z < 1$. In Eq. (2) we replace z and ωt by two sets of site-dependent functions $z_n(t)$ and $\varphi_n(t)$, respectively, which are assumed to vary slowly over a distance a . As shown in Sec. II, in a second order approximation scheme we obtain an EOM of the form

$$\begin{aligned} \frac{\partial \mathbf{S}}{\partial t} = & \left[B + (1 - \cos q) (\mathbf{e} \cdot (2\mathbf{S} + a^2 \frac{\partial^2 \mathbf{S}}{\partial x^2})) \right] \mathbf{S} \times \mathbf{e} \\ & - 2a \sin q (\mathbf{e} \cdot \mathbf{S}) \frac{\partial \mathbf{S}}{\partial x} \\ & + a^2 \cos q \mathbf{S} \times \frac{\partial^2 \mathbf{S}}{\partial x^2}. \end{aligned} \quad (5)$$

In the limit $q \rightarrow 0$, on rescaling the coordinate x , this equation reduces to the Landau-Lifshitz equation,

$$\frac{\partial \mathbf{S}}{\partial t} = \mathbf{S} \times \left(\frac{\partial^2 \mathbf{S}}{\partial x^2} + \mathbf{B} \right), \quad (6)$$

and hence Eq. (5) can be considered as the generalization of Eq. (6). As we show below Eq. (5) possesses one-soliton solutions, even if B equals 0, and probably also \mathcal{N} -soliton solutions.

The rationale for our strategy of developing Eq. (5) is as follows: The replacement of the finite difference expression $\mathbf{s}_{n+1} + \mathbf{s}_{n-1} - 2\mathbf{s}_n$ in Eq. (1) by the single term $\frac{\partial^2 \mathbf{S}}{\partial x^2}$, as in Eq. (6), is accurate as long as the continuous function $\mathbf{S}(x, t)$ varies sufficiently slowly over a distance a so that the effects of an infinite number of higher order spatial derivatives can be neglected. In particular, the solutions of the Landau-Lifshitz equation can only describe small deviations from spin wave solutions with q approximately zero. By contrast Eq. (5) starts from the expressions of Eq. (2) for any choice of q allowed by Eq. (3).

A first order version of the continuum EOM of Eq. (5), as shown in Sec. III, can be solved completely. Its solutions do not describe solitons but deformations of the initial profile similar to those of the Hamilton-Jacobi equation for free particles. After a finite time caustics are necessarily formed indicating that the first order approximation breaks down. In our numerical studies of Eq. (1) we do find instances where smooth or "laminar" solutions give way to a chaotic or "turbulent" regime, but this does not occur in general.

Solitons appear in the second order approximation of the EOM of Eq. (5). Using a discretized version of the initial form of a solution of Eq. (5), we find that, under certain conditions, the time-evolved numerical solution of the discrete spin EOM closely tracks the time-evolved solution. We call these numerical solutions "quasi-solitons". However, we have found that, in the case of $B = 0$, the existence of quasi-solitons is limited to a small "window" of q -values, say $\frac{6\pi}{N} < |q| < \frac{20\pi}{N}$ for

$N = 100$. Were we not guided by the solutions of the continuum equation, the chance of successfully generating a quasi-soliton solution to the discrete EOM is much like the proverbial "finding a needle in the haystack". In support of this, we find that for virtually all other choices of an initially localized spin configuration the spin pattern spreads with time and does not reassemble, let alone maintain its localized shape. This also applies to the first order approximation of the EOM, where we have also found numerical solutions that closely follow the initial stages of the evolution towards a caustic.

It is remarkable that the dynamical behavior of a relatively small number of interacting spins is so multi-faceted and unexpectedly rich, and that one is dependent on a study of the continuum version of the EOM to provide the key for unraveling and elucidating the dynamical properties of the discrete EOM. We have not attempted to analyze the third order version of the continuum EOM due to the severe mathematical complications that arise. Other interesting dynamical behavior, as yet unknown to us, might still be found from a deeper mathematical analysis of the complete continuum EOM.

Another important aspect is the question of how robust quasi-solitons are. One possible perturbation of solitons is the coupling of the spins to a heat bath. This kind of thermal perturbation is incorporated in our numerical treatment of the discrete EOM in Sec. VI. Likewise, we explore rings with relatively small values of N . We find that quasi-soliton solutions are relatively robust, surviving as long-lived spatially localized patterns as the temperature is increased and/or the initial profile is truncated or as N is decreased to as small as 11.

The kind of quasi-solitons investigated in the present paper represent only a certain fraction of solitary phenomena in spin systems known from the literature. Another class of solitons exists for classical chains with a particular form of anisotropy that leads to the Sine-Gordon equation [8]. Other soliton solutions for continuous EOM describing similar systems have been given in [9]-[12]. Solitary solutions of a quantum spin chain have been investigated, for example, in [13]. A very large literature (see [8] for a comprehensive review) exists which has shown that these EOM are of direct relevance to a wide class of one-dimensional magnetic materials and provide a variety of theoretical models in quantum field theory.

The layout of this paper is as follows. In Sec. II, starting from the discrete EOM for the interacting spin system, Eq. (1), we review the well-known exact spin-wave solutions, and then proceed to derive a continuum version of the EOM describing modulated spin waves. Sec. III is devoted to deriving the full set of solutions of the first order version of the continuum

EOM, and in particular to showing that any solution necessarily develops a caustic in the course of time. We include examples of numerical solutions of Eq. (1) showing such behavior. In Sec. IV we give a detailed analysis of the soliton solutions of the second order version of the continuum EOM. We obtain a formula for the dependence of the soliton amplitude A on the wave number q , the soliton velocity u , and the magnetic field B . In the limit $q \rightarrow 0$ this formula reduces to the well-known result for the Landau-Lifshitz equation. In Sec. V we present results of our numerical analysis of the discrete EOM of Eq. (1). These include one-quasi-solitons and multiple-quasi-solitons starting from initial profiles obtained from soliton solutions of the second order continuum EOM. Sec. VI is devoted to the effects of starting from initial spin configurations that are truncated versions of soliton states, as well as including the coupling of the discrete spins to a heat bath. Finally, in Sec. VII we summarize our results and discuss open questions.

II. MODULATED SPIN WAVES

We consider classical spin rings with N spins interacting via ferromagnetic nearest-neighbor coupling. The equations of motion are given by Eq. (1) where $\mathbf{B} = B\mathbf{e}$ is the dimensionless magnetic field and \mathbf{e} is chosen as a unit vector in the direction of the 3-axis. Mathematically, the case of anti-ferromagnetic coupling is included since it can be achieved by the transformation $\mathbf{s}_n \mapsto -\mathbf{s}_n$. However, solitons which are excitations of a background of fully aligned spins will be thermodynamically stable only in the ferromagnetic case. Hence we will stick to the ferromagnetic case for physical reasons. For $N > 4$ the general solution of Eq. (1) cannot be given in closed form. However, as mentioned above, there exist spin wave solutions of the form of Eq. (2). These solutions are parameterized by a variable z , the common 3-component of all spin vectors, and by the wave number q which assumes the discrete values of Eq. (3).

In this article we will consider modulations of Eq. (2) where z and ωt are replaced by two sets of functions $z_n(t)$ and $\varphi_n(t)$, respectively, which are assumed to vary slowly over a distance a . That is, $\mathbf{s}_n(t)$ is given by

$$\mathbf{s}_n(t) = \begin{pmatrix} \sqrt{1 - z_n(t)^2} \cos(qn - Bt - \varphi_n(t)) \\ \sqrt{1 - z_n(t)^2} \sin(qn - Bt - \varphi_n(t)) \\ z_n(t) \end{pmatrix} \quad (7)$$

It is convenient to remove the term qn by the transformation

$$\tilde{\mathbf{s}}_n(t) \equiv R_3(-qn) \mathbf{s}_n(t), \quad (8)$$

where $R_3(\alpha)$ denotes the matrix of a rotation about the 3-axis with an angle α . One could also remove the

magnetic field by a suitable uniform rotation but we prefer to retain B in what follows in order to make the transition to the Landau-Lifshitz equation more transparent.

In the continuum approximation we introduce smooth functions $z(x,t)$, $\varphi(x,t)$ and $\mathbf{S}(x,t)$ such that $z(na,t) = z_n(t)$ and $\varphi(na,t) = \varphi_n(t)$, and

$$\mathbf{S}(x,t) = \tilde{\mathbf{s}}_{x/a}(t) = \begin{pmatrix} \sqrt{1 - z(x,t)^2} \cos(Bt + \varphi(x,t)) \\ -\sqrt{1 - z(x,t)^2} \sin(Bt + \varphi(x,t)) \\ z(x,t) \end{pmatrix} \quad (9)$$

In the continuum approximation we allow for the parameter q to take on any values in the interval $(-\pi, \pi)$, whereas the Landau-Lifshitz equation is obtained in the limit $q \rightarrow 0$.

Using the addition theorems for cos and sin we obtain

$$\mathbf{s}_{n\pm 1} = \begin{pmatrix} \sqrt{1 - z_{n\pm 1}^2} [\cos \alpha_{\pm} \cos q \mp \sin \alpha_{\pm} \sin q] \\ \sqrt{1 - z_{n\pm 1}^2} [\sin \alpha_{\pm} \cos q \pm \cos \alpha_{\pm} \sin q] \\ z_{n\pm 1}(t) \end{pmatrix} \quad (10)$$

where

$$\alpha_{\pm} \equiv qn - Bt - \varphi_{n\pm 1}(t). \quad (11)$$

Applying the rotation $R_3(-qn)$ to $\mathbf{s}_{n+1} + \mathbf{s}_{n-1}$ hence yields

$$\begin{aligned} R_3(-qn)(\mathbf{s}_{n+1} + \mathbf{s}_{n-1}) = & (\tilde{\mathbf{s}}_{n+1} + \tilde{\mathbf{s}}_{n-1}) \cos q \\ & + \mathbf{e} \times (\tilde{\mathbf{s}}_{n+1} - \tilde{\mathbf{s}}_{n-1}) \sin q \\ & + (z_{n+1} + z_{n-1})(1 - \cos q)\mathbf{e}. \end{aligned} \quad (12)$$

Finally, we use the representation of Eq. (9) and apply the rotation $R_3(-qn)$ to the EOM of Eq. (1) thus obtaining the continuum approximation of the form

$$\frac{\partial}{\partial t} \mathbf{S}(x,t) = \mathbf{S}(x,t) \times \mathbf{H}(x,t), \quad (13)$$

where

$$\begin{aligned} \mathbf{H}(x,t) = & [(\mathbf{S}(x+a,t) + \mathbf{S}(x-a,t))] \cos q \\ & + \mathbf{e} \times [\mathbf{S}(x+a,t) - \mathbf{S}(x-a,t)] \sin q \\ & + [B + (z(x+a,t) + z(x-a,t))(1 - \cos q)] \mathbf{e}. \end{aligned} \quad (14)$$

In the following we consider truncated versions of Eqs. (13) and (14). These are obtained by first expanding $\mathbf{S}(x \pm a, t)$ in powers of a . We obtain an infinite order partial differential equation (PDE) of the form of Eq. (13)

with

$$\begin{aligned} \mathbf{H} &= 2 \left(\mathbf{S} + \frac{a^2}{2} \mathbf{S}'' + \frac{a^4}{4!} \mathbf{S}^{(4)} + \dots \right) \cos q \\ &+ 2\mathbf{e} \times \left(a\mathbf{S}' + \frac{a^3}{3!} \mathbf{S}^{(3)} + \dots \right) \sin q \\ &+ \left[B + 2 \left(z + \frac{a^2}{2} z'' + \frac{a^4}{4!} z^{(4)} + \dots \right) (1 - \cos q) \right] \mathbf{e}, \end{aligned} \quad (15)$$

where the arguments (x, t) have been suppressed, and we abbreviate the spatial derivatives of \mathbf{S} and z by a prime and the time derivatives by a dot in what follows. In the n th order approximation we keep terms containing powers of a through a^n . In this article we consider zeroth, first, and second order approximations only. The 0th order PDE is given by

$$\dot{\mathbf{S}} = (B + 2z(1 - \cos q))\mathbf{S} \times \mathbf{e}. \quad (16)$$

This equation is solved by the spin wave solution, Eq. (2), but it also has more general solutions.

III. FIRST ORDER EQUATIONS

In the first order approximation Eqs. (13) and (15) reduce to

$$\dot{\mathbf{S}} = [B + 2(1 - \cos q)(\mathbf{e} \cdot \mathbf{S})] \mathbf{S} \times \mathbf{e} - 2a \sin q (\mathbf{e} \cdot \mathbf{S}) \mathbf{S}'. \quad (17)$$

Using the representation of Eq. (9) we can rewrite this equation as

$$\dot{\varphi} = B + 2z(x, t)((1 - \cos q) - a \sin q \varphi') \quad (18)$$

$$\dot{z} = -2a \sin q z z'. \quad (19)$$

First we consider Eq. (19), which is an autonomous equation for $z(x, t)$. Its solution is well-known, see e. g. [14]. Equation (19) essentially describes the velocity field of a system of free particles with a given velocity distribution for $t = 0$. To make this more transparent, consider the transformation

$$v(x, t) \equiv z\left(x, \frac{t}{2a \sin q}\right), \quad (20)$$

which transforms Eq. (19) into

$$\dot{v} + vv' = 0. \quad (21)$$

Hence v is constant along the lines with slope $\frac{dx}{dt} = v$ whence the above kinematical interpretation follows. Let $\xi = x - vt$ be the x -coordinate of the intersection of the axis $t = 0$ and the line through the point (x, t) with slope u . Hence $u = v(\xi, 0)$. This yields a parametric representation of the graph of the general solution $x \mapsto v(x, t)$ of Eq. (21) for fixed t , namely

$$x = \xi + v(\xi, 0)t \quad (22)$$

$$u = v(\xi, 0), \quad (23)$$

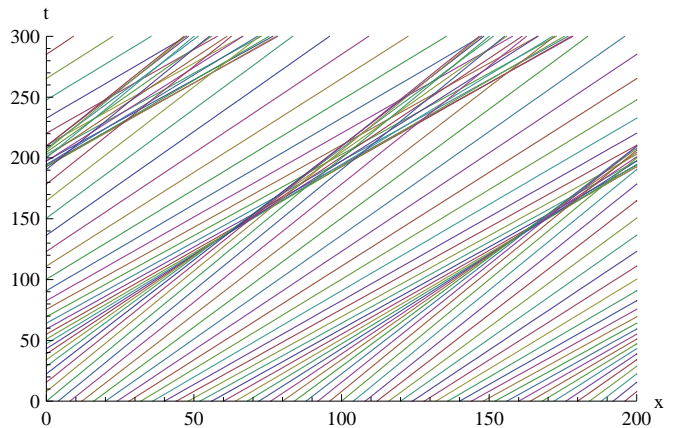


FIG. 1: Caustics in a line field with initial slope $v(x, 0) = \frac{1}{2} + \frac{1}{4} \sin^2\left(\frac{\pi x}{100}\right)$.

where $v(\xi, 0)$ is an arbitrary initial condition for the considered PDE. An example of the resulting line field is given in Fig. 1. We see that there are domains, where the lines in the line field intersect, bounded by curves called “caustics”. These domains correspond to points where the parametric representation of Eqs. (22), (23) defines a multi-valued function. The earliest time when caustics appear is given by

$$t_c = -\frac{1}{\frac{\partial v(\xi_0, 0)}{\partial \xi}}, \quad (24)$$

where ξ_0 is the point with the largest negative derivative of $v(\xi, 0)$. Initial profiles $v(\xi, 0)$ with only positive slope do not have caustics for $t > 0$ but cannot be realized on a spin ring with periodic boundary conditions.

The same analysis applies to the original equation Eq. (19), except that the caustic time t_c in Eq. (24) has to be divided by $2a \sin q$. Hence the first order PDE predicts that after some time t_c the profile of the 3-components of the spin ring develops an infinite slope. That is for later times the 1st order analysis is no longer valid and the equations of motion must be studied by using higher order approximations. Remarkably, there exist examples where the numerical solution of Eq. (1) is well described by its 1st order approximation for times t with $0 \leq t < t_c$. Close to the time $t = t_c$ the smooth “laminar” time evolution breaks down and a different regime begins to penetrate the spin ring. We will call this regime “turbulent” for sake of simplicity, but we do not know whether it is genuinely chaotic or still regular on a shorter length scale. From our numerical results the latter cannot be excluded. Figure 2 shows the numerical solution $z_n(t)$ of Eq. (1) for an $N = 100$ spin ring with $q = 16\pi/100$, together with the 1st order PDE solution $z(x, t)$ at the time $t = t_c$. The two sets of results are in close agreement, although at time $t = t_c$ the continuum approximation is no longer applicable.

We remark that equation (18) can also be solved in

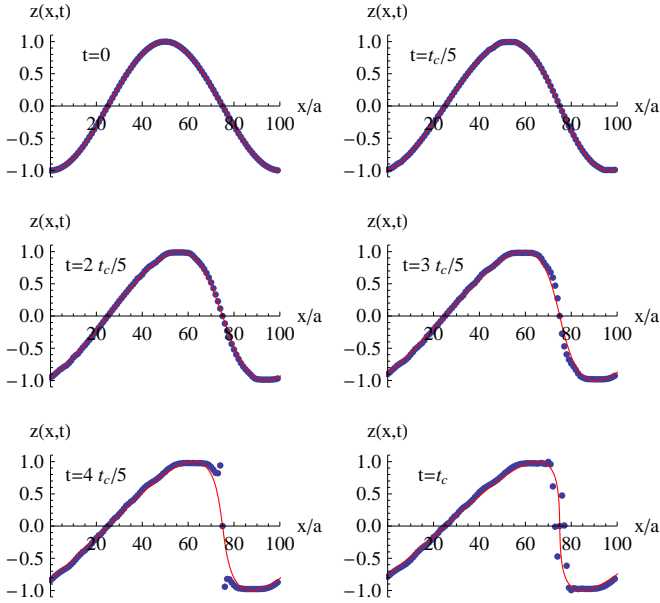


FIG. 2: Numerical solutions $z_n(t)$ of the discrete EOM of Eq. (1) for a spin ring with $N = 100$ (blue dots) and solution of the 1st order continuum approximation $z(x, t)$ (solid red curve), where $t = nt_c/5$, $n = 0, 1, \dots, 5$ and t_c is the caustic time defined in Eq. (24). For $t > t_c$ the solid curve bends over and defines a 3-valued function.

closed form. Its general solution utilizes the solution $z(x, t)$ of Eq. (19) already obtained and the initial angle distribution $\varphi_0(x) = \varphi(x, 0)$ and it is given by

$$\varphi(x, t) = \varphi_0(x - 2a \sin q z(x, t)t) + z(x, t)2(1 - \cos q)t + Bt. \quad (25)$$

Hence the effects of the caustics will also be manifested in the behavior of the azimuthal angles of the spin vectors.

IV. THE SECOND ORDER EQUATIONS

In the preceding section we have seen that the 1st order approximation predicts its own break-down since it will necessarily lead to a caustic or “turbulent” behavior. Hence the question arises whether higher order approximations give rise to the same or different effects. The second order equation is given by

$$\begin{aligned} \dot{\mathbf{S}} &= [B + 2(1 - \cos q)(\mathbf{e} \cdot \mathbf{S})] \mathbf{S} \times \mathbf{e} \\ &- 2a \sin q (\mathbf{e} \cdot \mathbf{S}) \mathbf{S}' \\ &+ a^2 \mathbf{S} \times [\cos q \mathbf{S}'' + (1 - \cos q)(\mathbf{e} \cdot \mathbf{S}) \mathbf{e}]. \end{aligned} \quad (26)$$

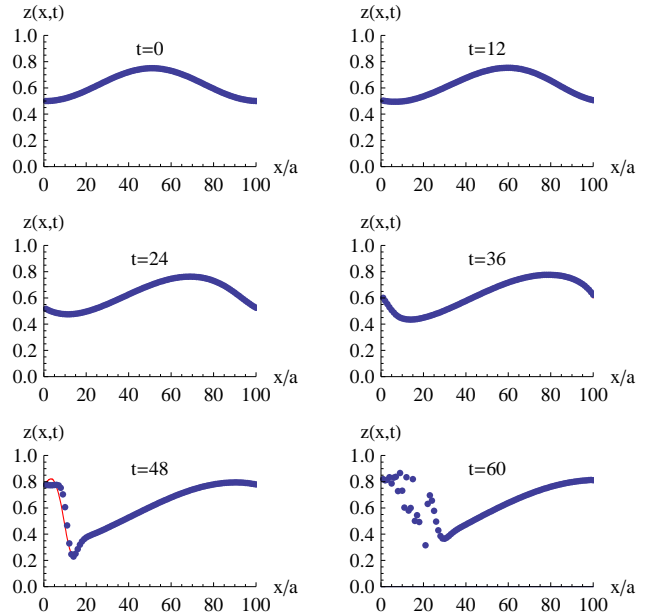


FIG. 3: Comparison of a numerical solution for $z_n(t)$ at fixed times $t = 0, 12, \dots, 60$ of the equations of motion for an $N = 100$ spin ring (blue dots) with the numerical solution of its 2nd order continuum approximation Eqs. (27), (28) (solid red curve) at the times $t = 0, 12, \dots, 48$. The turbulent regime begins to spread at approximately $t = 48$. By $t = 60$ the numerical solution breaks down and hence cannot be drawn.

Substituting Eq. (9) leads to

$$\begin{aligned} \dot{\varphi} &= B + 2z (1 - \cos q - a \sin q \varphi') \\ &+ a^2 \left[z'' + z \cos q \left(\varphi'^2 + \frac{z z''}{1 - z^2} + \frac{z'^2}{(1 - z^2)^2} \right) \right] \end{aligned} \quad (27)$$

$$\begin{aligned} \dot{z} &= -2a \sin q z z' \\ &+ a^2 \cos q (2z z' \varphi' - (1 - z^2) \varphi''). \end{aligned} \quad (28)$$

In solving Eq. (26) numerically and analytically we have found instances where the onset of turbulence is accelerated as well as where it is entirely suppressed. We do not, however, have a clear understanding about the underlying causes for either behavior. As an example of the first case, acceleration of turbulence, in Fig. 3 we compare results of the numerical solution of the EOM of Eq. (1) with the numerical solution of Eqs. (27) and (28). The time of the onset of the turbulence is approximately 2.75 times shorter than that predicted by the 1st order approximation.

The other case, preservation of laminar behavior, due to 2nd order effects, can be most impressively demonstrated by the existence of solitons, presented in the next subsection.

A. Exact single soliton solutions

The mathematical derivation of soliton solutions is to a large extent analogous to the Landau-Lifshitz case, see [4], [6]. To simplify the derivation we set $a = 1$ in the following.

We seek solutions of Eqs. (27) and (28) of the form

$$\varphi(x, t) = \Phi(x - ut) \quad (29)$$

$$z(x, t) = Z(x - ut). \quad (30)$$

The resulting equation for $Z(x)$ can be integrated once yielding

$$\Phi' = \sec q \frac{u(Z - Z_0) - Z^2 \sin q}{1 - Z^2}, \quad (31)$$

where Z_0 is some integration constant. Substituting this into the equation resulting from Eq. (27) yields a second order equation for $Z(x)$. Multiplying with $Z'(x)$ and integrating with respect to x yields an expression for $Z'(x)^2$ containing an integration constant c . This expression is analogous to a one-dimensional potential if $Z'(x)^2$ is viewed as the kinetic energy and the total energy is set equal to 0, namely

$$\begin{aligned} Z'^2 = -V(Z) &= \frac{1}{2(1 - Z^2(1 - \cos q))} \\ &\{ \sec q [-1 - 3Z^2 - 2u^2(2ZZ_0 - 1 - Z_0^2) \\ &- (1 + Z^2) \cos 2q + 8Z^2(1 - Z^2) \sin^4 \frac{q}{2}] \\ &+ 4 [c(Z^2 - 1) + Z(Z + B(1 - Z^2)) \\ &+ u(Z_0 - Z^3) \tan q] \}. \end{aligned} \quad (32)$$

$V(z)$ will be called the pseudo-potential. Since $-V(Z)$ is biquadratic in Z in the numerator and quadratic in the denominator the integral

$$x - x_0 = \int \frac{dZ}{\sqrt{-V(Z)}} \quad (33)$$

can be expressed in terms of elliptic functions of the first and third kind, see [17]. The inverse function of Eq. (33), together with the integral of Eq. (31), gives the inverse function of the soliton solution. However, the analytic expression is very complicated and it is far simpler to calculate the integral of Eq. (33) numerically. The poles of $V(Z)$ lie at $Z_p = \frac{\pm 1}{\sqrt{1 - \cos q}}$ and hence are outside the physical domain $Z \in [-1, 1]$ for $0 < |q| < \frac{\pi}{2}$. Hence we will assume

$$0 < |q| < \frac{\pi}{2} \quad (34)$$

in the following.

The remaining task is to determine values of the parameters q, B, u, Z_0, c for which solitary solutions of Eqs. (27) and (28) exist. The inverse function of (33)

has the form of a soliton profile if $V(Z)$ has a double root at $Z = Z_1$ and a simple root at $Z = Z_2$ such that $-1 \leq Z_1 < Z_2 \leq 1$ and $V(Z)$ is negative in the interval (Z_1, Z_2) . For sake of simplicity we only consider the case $Z_1 = -1$.

The condition that $V(Z)$ has a double root at $Z = Z_1 = -1$ gives us two parameters as a function of the remaining two:

$$c = 1 - B - \frac{(2 + Z_0)^2 \cos q + (Z_0^2 - 2) \sec q}{4 \cos q (1 + Z_0)^2} \quad (35)$$

$$u = -\frac{\sin q}{1 + Z_0}. \quad (36)$$

The soliton solutions hence depend on three parameters which we choose to be B, q and u . A typical form of $V(Z)$ is shown in Fig. 4. For the numerical studies in Sec. V and VI we mostly chose negative wave-numbers q in order to get positive velocities according to Eq. (36).

The remaining roots $Z_{2,3}$ are

$$\begin{aligned} Z_{2,3} &= \frac{1}{8} \csc^4 \frac{q}{2} [3 + \cos 2q + 2u \sin q \\ &- 2 \cos q (2 - B \mp f(B, q, u))] \end{aligned} \quad (37)$$

where

$$f(B, q, u) \equiv \sqrt{B^2 - 2u^2 + 2u \sec q (u + B \sin q)}. \quad (38)$$

The condition that $V(Z)$ is negative in the interval $Z \in (-1, Z_2)$ or, equivalently, $V''(-1) < 0$, which is necessary for the existence of solitons, leads to the inequalities

$$\begin{aligned} -2 \sin q - 2 \cos q \sqrt{(2 - B) \sec q - 2} \\ < u < \end{aligned} \quad (39)$$

$$-2 \sin q + 2 \cos q \sqrt{(2 - B) \sec q - 2}$$

This defines a certain physical domain in the (B, q, u) -plane, see Fig. 5, where solitons exist. It is bounded by $B \leq 2$. The inequalities further imply that only the root Z_2 of $V(Z)$ with the $-$ sign in Eq. (37) lies inside the physical domain $(-1, 1)$.

Eq. (37) yields an explicit relation between the amplitude $A \equiv Z_2 - Z_1 = 1 + Z_2$ and the velocity u of the soliton of the form

$$A = 2 + \frac{u \sin q + (B + f(B, q, u)) \cos q}{4 \sin^4 \frac{q}{2}}, \quad (40)$$

with $f(B, q, u)$ defined by Eq. (38). The two limiting forms are

$$A = 2 + \frac{u^2}{2B} \text{ for } q \rightarrow 0 \text{ and } B < 0, \quad (41)$$

to be compared to Eq. (4.7) in [6], and

$$\begin{aligned} A &= 2 + \frac{1}{4} \csc \frac{q}{2} \left(u \sin q - |u| \sqrt{2(\sec q - 1) \cos q} \right) \\ &\text{for } B \rightarrow 0. \end{aligned} \quad (42)$$

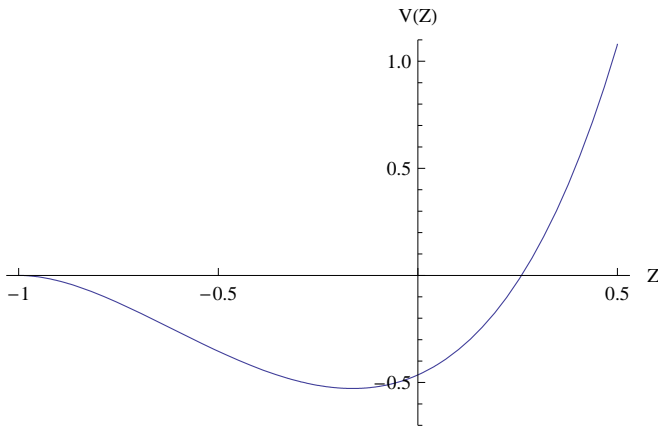


FIG. 4: The pseudo-potential $V(Z)$ according to Eq. (32) corresponding to the parameters $B = 0$, $q = -\pi/4$ and $u = 1$.

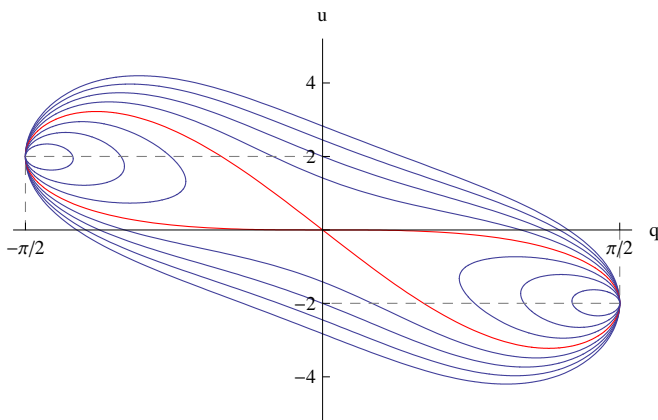


FIG. 5: The soliton velocities u bounded by a function of q and B according to Eq. (39). Curves shown correspond to $B = -2, -1.5, \dots, 1.5$. The ∞ -shaped red curve corresponds to $B = 0$. For $B \rightarrow 2$ the curves shrink to two points at $q = \pm\pi/2$, $u = \mp 2$.

The physical part of the surface in (q, u, A) -space spanned by the lines defined by Eq. (42) with $q = \text{const.}$ is shown in Fig. 6. From these equations it follows that the amplitude A diverges for $B, q \rightarrow 0$ and hence no solitons exist in this case in accordance with [6].

V. NUMERICAL SOLITON SOLUTIONS

In this section we summarize some of our results for numerical solutions of the EOM, Eq. (1), in the case $B = 0$, for finite spin rings. The initial spin configurations are selected to be soliton profiles as calculated from the 2nd order continuum PDE using Eqs. (31) - (33). Fig. 7 shows the initial profile of a discrete soliton for a spin ring with $N = 100$ and parameters $q = -8\pi/100$ and $u = -\sin q$. The soliton appears as a localized deviation from an otherwise ferromagnetic alignment of spins. Using this initial profile we solve

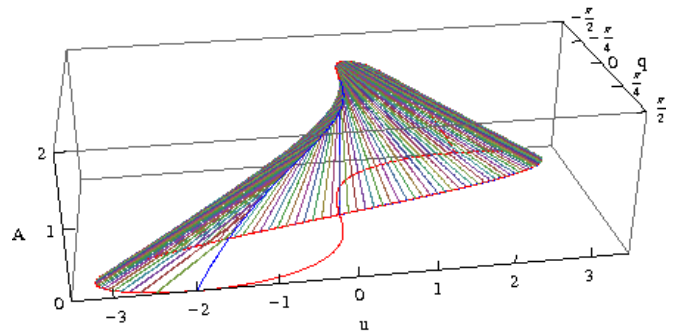


FIG. 6: Soliton amplitude A as a function of wave number q and velocity U for $B = 0$ according to Eq. (42).

the EOM, Eq. (1), numerically to determine the time evolution of the spin vectors. The results are shown in Fig. 8. In panel a) we provide a snapshot of $z_n(t)$ for a particular time $t = 2000$. A comprehensive picture for all calculated times is given in the color contour plot of panel b), where the color gives the value of $z_n(t)$ according to the coding defined in the legend. The strict integrity of the solution as a function of time is striking. Throughout the remainder of this paper we use color contour plots since they provide a very effective tool for visualizing the overall time evolution of the spin profile as measured by $z_n(t)$. In particular, these plots allow one to detect even small changes in the profile, its speed, etc.

Using the initial profile for a single soliton solution it is easy to prepare the case of two identical solitons moving towards each other. We copy the single soliton profile of the $N = 100$ spin ring onto one half of an $N = 200$ spin ring and its reversed version onto the second half of the spin ring. As is seen in Fig. 9, the numerical solution of Eq. (1) describes two solitons that collide and then move apart while retaining their initial shapes and velocities. This behavior is well-known for exact \mathcal{N} -soliton solutions of other nonlinear wave equations, see, e. g. [17]. We have observed repeated collisions of the soliton pairs without noticeable deformation. By using a similar procedure we have created the situation where a faster soliton overtakes a slower one, and the results are shown in Fig. 10. One can see that the penetration of the slower soliton by the faster one does not alter the shape or velocity of either soliton subsequent to their collision.

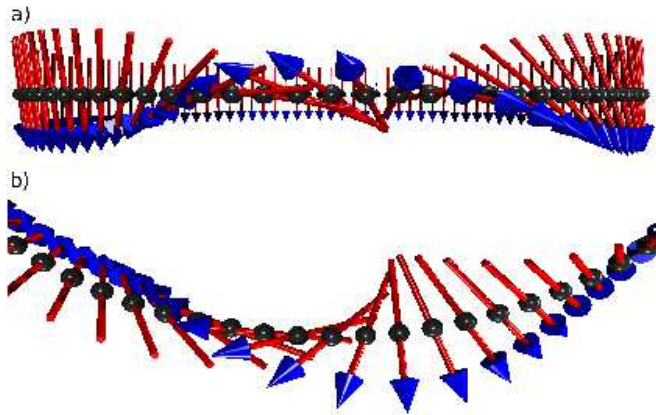


FIG. 7: Initial profile of a discrete soliton for a spin ring with $N = 100$ calculated from Eqs. (31) - (33) for parameters $q = -8\pi/100$ and $u = \sin|q|$. Panel a) shows the in-plane view while panel b) shows the structure of the soliton as viewed from above. The initial profile $z_n(t)$ can be traced by eye following the blue arrow tips. The time evolution of this soliton is shown in Fig. 8.

VI. EFFECTS OF TRUNCATION AND FINITE TEMPERATURE

The purpose of this Section is to explore the extent to which quasi-solitons are robust to various perturbations. We begin by investigating the time evolution of symmetrically truncated versions of initial states that exhibit soliton behavior. This is illustrated schematically in Fig. 11, where the black dots describe a hypothetical non-truncated initial profile. In the truncated version, for all but M spins the value of $z_n(0)$ is set equal to -1 , whereas we retain the original values of $z_n(0)$ for the M spins. The latter are chosen to be centered about the site having the largest value of $z_n(0)$.

Based on the initial profile used for the soliton shown in Fig. 8 we have used $M = 10$ as well as $M = 3$ for the corresponding truncated versions. As shown in Figs. 12 and 13, soliton behavior is clearly maintained for the choice $M = 10$ and surprisingly, despite the fact that this is a nonlinear problem, even for $M = 3$. For the case $M = 3$ there is only an increased level of background noise while the major features of the quasi-soliton are retained.

While our quasi-soliton solutions appear to be robust against *symmetric* truncation we have found that *asymmetric* off-center truncation leads to far less stable behavior, i. e. , the soliton decays after some time which depends on the extent of the asymmetry.

Another way of truncating the initial profile is to reduce the system size N , but leaving the initial profile intact. This means, that for the system sizes where

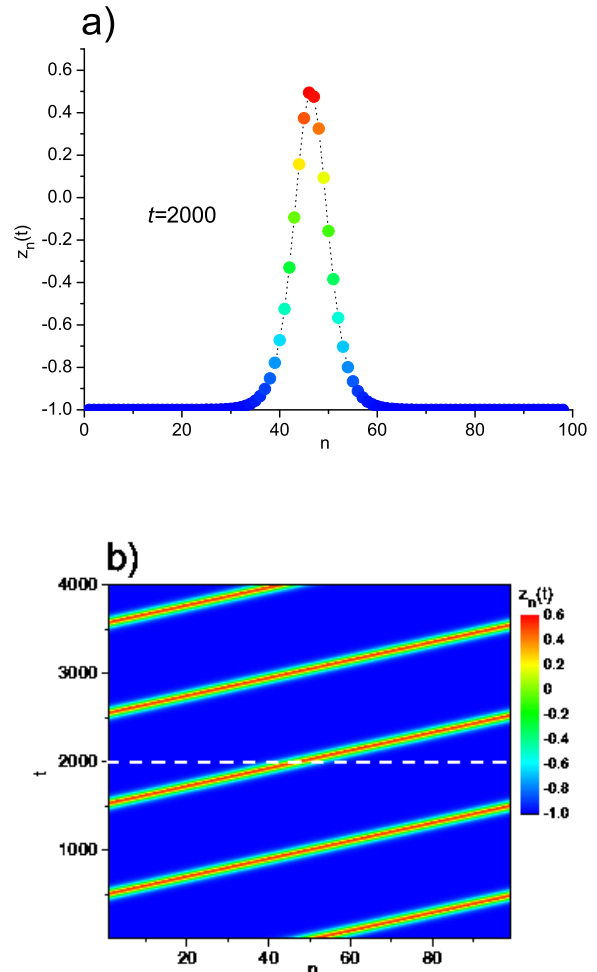


FIG. 8: Time evolution of the discrete soliton with initial profile shown in Fig. 7. Panel a) shows a snapshot of the values of $z_n(t)$ for $t = 2000$. The color coding corresponds to the contour plot given in panel b). The data given in panel a) correspond to the dashed white line shown in panel b).

$N < M$ the truncation effects are due to the imposed cyclic boundary conditions. Our study is based on the numerical solution $z_n(t)$ with the initial data calculated from Eqs. (31) - (33) using the parameters $q = -32\pi/100$ and $u = \sin|q|$. In Fig. 14 we show results for a spin ring with $N = 20$. The initial profile is symmetrically truncated around the maximum value of $z_n(t)$. One clearly sees soliton behavior with some background noise and a slight pulsation of the amplitude $z_n(t)$. By reducing the system size to $N = 11$ spins soliton behavior is still visible, however the pulsation of the amplitude is strongly enhanced (see Fig. 15).

While in all of the above cases the total energy is a conserved quantity we now show one specific example of the behavior of the quasi-solitons when the spin system is coupled to a heat bath. The behavior of classical spin

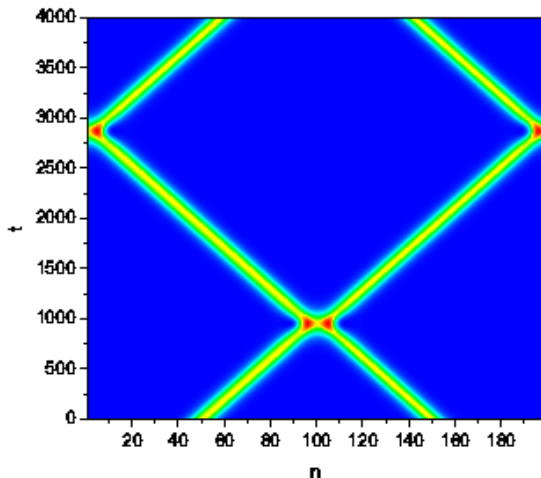


FIG. 9: Collision of two solitons of an $N = 200$ spin ring. The initial profile has been calculated from Eqs. (31) - (33) using the parameters $q = \pm 16\pi/200$ and $u = -\sin q$. The numerical solutions are displayed for $t = 0, \dots, 4000$, including the times $t_1 \approx 1000$ and $t_2 \approx 2800$ where collision between the two solitons take place.

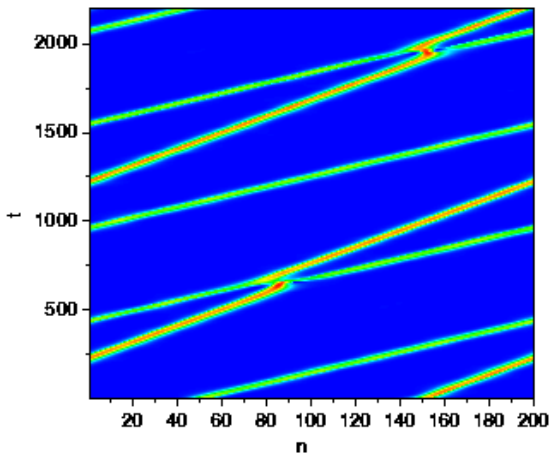


FIG. 10: Numerical two-soliton solution $z_n(t)$ for an $N = 200$ spin ring and initial data calculated from Eqs. (31) - (33) using the parameters $q = -16\pi/200$ and $u = 0.625 \sin |q|$ resp. $u = 1.25 \sin |q|$. The solution is displayed for $t = 0, \dots, 2200$. In this case two solitons are created which move in the same direction while one soliton is twice faster than the other eventually penetrating the slower one.

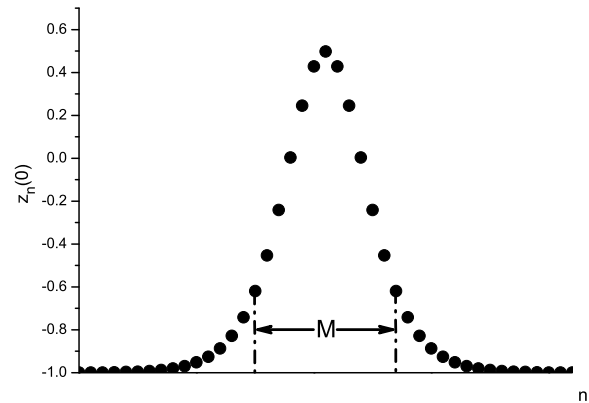


FIG. 11: Non-truncated initial profile (black dots) and truncated initial profile which is obtained by taking out M spins centered about the site having the largest value of $z_n(0)$ and setting the value of $z_n(0)$ equal to -1 for the remaining spins.

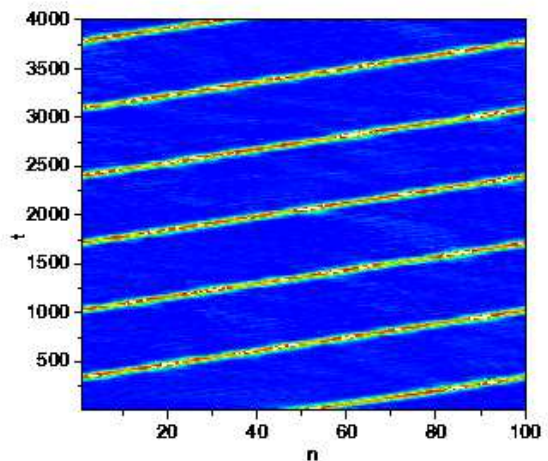


FIG. 12: Time evolution for an $N = 100$ spin ring and an initial profile, schematically described by Fig. 11, where $M = 10$ spin vectors are specified as in Fig. 7 and the remaining 90 spin vectors are initially set anti-parallel to the 3-axis.

systems in contact with a heat bath can very effectively be studied using a constant temperature stochastic spin dynamics approach, such as that used in [5] [16]. Here the spin system is coupled to a heat bath according to a Langevin-type approach by including a Landau-Lifshitz damping term as well as a fluctuating force with white noise characteristics.

Starting from prescribed initial conditions as those used in Fig. 8 the temperature is set to a value $T > 0$ and the trajectory of the system is calculated numerically by

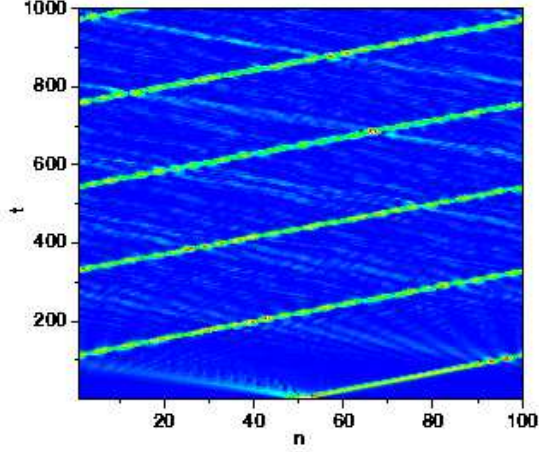


FIG. 13: Time evolution for an $N = 100$ spin ring and an initial profile, schematically described by Fig. 11, where only $M = 3$ spin vectors are specified as in Fig. 7 and the remaining 97 spin vectors are initially set parallel to the z -axis. Even in this case a rather stable quasi-soliton is created. However, with its generation a small localized perturbation appears which moves in the opposite direction. Its interference with the quasi-soliton can be observed several times (first at time $t \approx 100$).

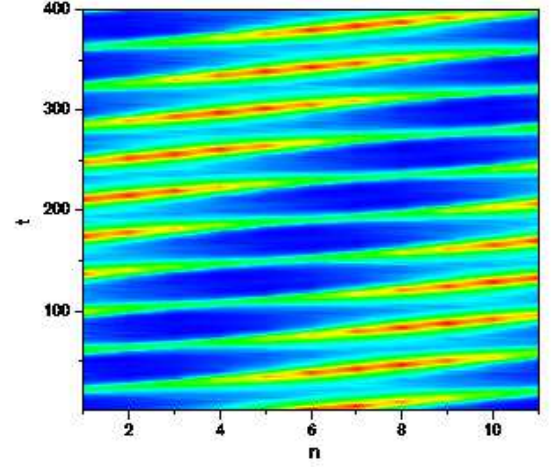


FIG. 15: Time evolution for an $N = 11$ spin ring, where the initial data are selected as described in the text. While some features of soliton-like behavior are still visible, because of the small value of N the results are strongly affected by background noise and pulsation of the amplitude $z_n(t)$.

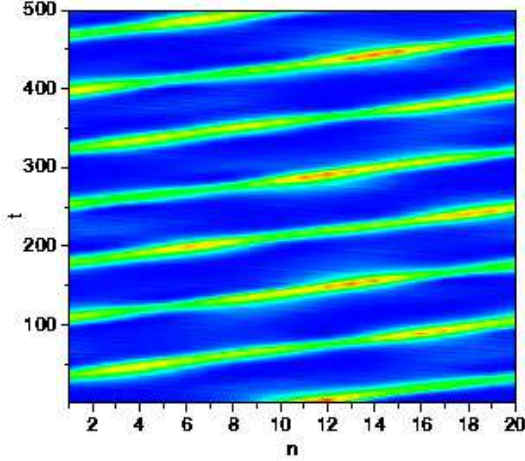


FIG. 14: Time evolution for an $N = 20$ spin ring, where the initial data are selected as described in the text. Soliton-like behavior persists although some background noise and pulsation of the amplitude $z_n(t)$ is visible.

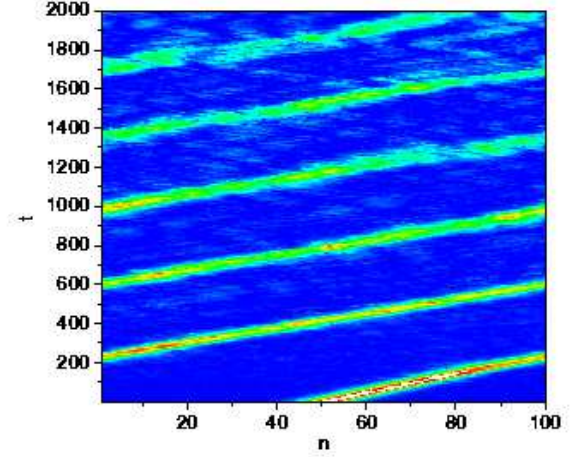


FIG. 16: Finite temperature effects on a quasi-soliton solution $z_n(t)$ for an $N = 100$ spin ring and initial data calculated from Eqs. (31) - (33) using the parameters $q = -8\pi/100$ and $u = \sin|q|$. Compared to the $T = 0$ case shown in Fig. 8 one observes that thermal fluctuations lead to a decay of the soliton, however, it persists for a significant length of time before eventually dissipating.

solving a stochastic Landau-Lifshitz equation, thereby allowing the spin system to exchange energy with its environment [5] [16]. Our results are shown in Fig. 16. Thermal fluctuations lead to a decay of the quasi-soliton, driving the system towards its (ferromagnetic) equilibrium configuration. However, the soliton persists for a significant length of time before eventually dissipating, as expected.

The cases considered in this Section provide a picture of quasi-solitons in classical Heisenberg rings that are remarkably robust even when perturbed by truncations, small system size, and heat bath couplings.

VII. SUMMARY

The overriding theme of this paper is that relatively small classical Heisenberg rings exhibit a rich variety of dynamical properties including soliton behavior. We have proposed that an effective strategy for exploring the dynamical behavior of these rings is to solve the system of discrete EOM of Eq. (1) upon selecting initial spin configurations that are discretized versions of the solutions of a new continuum EOM that we derived by allowing for continuous modulations of the spin wave solutions given by Eq. (2). In practice, due to the complexity of the analysis, we have limited our analysis to a second order PDE version, Eq. (26), of the continuous EOM of Eqs. (13) and (14). This second order PDE is a generalization of the Landau-Lifshitz equation that has been used extensively in studying one-dimensional magnetic systems, e. g. , spin chains. Among the class of solutions of Eq. (26) we have found soliton solutions. Using discretized versions of the soliton solutions as input data, we have found that the discrete EOM of Eq. (1) possess quasi-soliton solutions. The robustness of these discrete quasi-solitons has been demonstrated both by considering truncated versions of continuum soliton solutions as well as by investigating

the dynamical behavior when the spins are coupled to a heat bath at finite temperatures. Apart from quasi-soliton behavior there is a vast diversity of other dynamical behavior exhibited by finite spin rings. We have only sparsely investigated this diversity, and at present we have only a limited physical understanding of the behavior we have observed. We conjecture that the existence of robust quasi-solitons can be explained by the existence of exact solitary solutions of Eq. (1), i. e. , localized solutions satisfying $\mathbf{s}_{n+1}(t+T) = \mathbf{s}_n(t)$ for all $n = 1, \dots, N$ and some fixed T .

Magnetic solitons have been detected in many magnetic systems through their signature on such observables as specific heat, NMR, and neutron scattering [8]. Apart from any intrinsic interest in the dynamics of classical Heisenberg spin rings, we were motivated to undertake the present study as a first step in considering their quantum analogues. This is especially relevant in view of the rapidly growing number of quantum spin rings that are now available in the form of synthesized magnetic molecules [1] - [3]. It is thus timely to ask what is the quantum analogue of solitons in ring systems, and how might these be detected by experiment [13]?

Acknowledgements

Ch. Schröder is grateful to the University of Applied Sciences Bielefeld for financial support. Work at the Ames Laboratory was supported by the Department of Energy-Basic Energy Sciences under Contract No. DE-AC02-07CH11358. We thank Paul Sacks of Iowa State University's Department of Mathematics for useful discussions on Lax pairs and \mathcal{N} -soliton solutions. H.-J. Schmidt thanks Ames Laboratory for funding an extended visit to Ames where much of this research was performed.

-
- [1] D. Gatteschi, R. Sessoli, and J. Villain, *Molecular Nanomagnets* (Oxford Press, New York, 2006).
 - [2] R. E. P. Winpenny, J. Chem. Soc. Dalton Trans. **1**, 1 (2002).
 - [3] R. E. P. Winpenny, Comp. Coord. Chem. II **7**, 125 (2004).
 - [4] D. C. Mattis, *The theory of magnetism I*, 2nd ed., Springer, Berlin, Heidelberg, New York (1988).
 - [5] Ch. Schröder, PhD Dissertation, Universität Osnabrück (1999).
 - [6] H. C. Fogedby, J. Phys. A: Math. Gen. **13**, 1467 (1980).
 - [7] L. D. Landau, E. M. Lifshitz, Phys. Z. Sowjet. **8**, 153 (1935).
 - [8] H.-J. Mikeska and M. Steiner, Adv. Phys. **40**, 191 (1991).
 - [9] H. Yue, X. -J. Chen, and N. N. Huang, J. Phys. A: Math. Gen. **30**, 2491-2501 (1997).
 - [10] M. Daniel and L. Kavitha, Phys. Rev. B **59**, 13774-13776 (1999).
 - [11] X. -J. Chen and W. K. Lam Phys. Rev. E **69**, 066604 (2004).
 - [12] E. G. Galkina, A. Yu. Galkin, and B. A. Ivanov, arXiv:cond-mat/0712.0073.
 - [13] J. Schnack and P. Shchelokovskyy, J. Magn. Magn. - Mater. **306**, 79 (2006).
 - [14] G. B. Whitham, *Linear and Nonlinear Waves*, Wiley, New York (1974), Chap. 2.
 - [17] M. J. Ablowitz and H. Segur, *Solitons and the inverse scattering transform*, SIAM, Philadelphia (1981).
 - [16] V. A. Antropov, S. V. Tret'yakov, and B. N. Harmon, J. Appl. Phys. **81**, 3961 (1997).

- [17] M. Abramowitz and I. A. Stegun (eds.), *Handbook of Mathematical Functions*, Dover, New York (1965). at <http://spin.fh-bielefeld.de> .
- [18] We invite the reader to examine movies of our simulations